Available online at www.sciencedirect.com
ScienceDirect
Energy Procedia 69 (2015) 3 – 13
Energy Procedia

International Conference on Concentrating Solar Power and Chemical Energy Systems, SolarPACES 2014

Thermal stress analysis of absorber tube for a parabolic collector under quasi-steady state condition

M. H. Abedini-Sanigy[a], F. Ahmadi[b], E. Goshtasbirad[c], M. Yaghoubi[d,]*

[a,b]*M.Sc., Mechanical Engineering Department, Shiraz University, Mollasadra Street, Shiraz, Iran*
[c]*Assistant Prof., Mechanical Engineering Department, Shiraz University, Mollasadra Street, Shiraz, Iran*
[d]*Prof., Mechanical Engineering Department, Shiraz University, Mollasadra Street, Shiraz, Iran*

Abstract

The design of parabolic trough collectors is based on the concentration of solar heat flux on its absorber tube. This may be subjected to high thermal stresses which could cause deflection of the absorber tube and failure of its cover glass tube. Investigation of earlier studies on thermal gradient and thermal stresses demonstrates that so far, the issue is considered for steady state condition based on the assumption of constant solar heat flux distribution during the day hours. However, in practice, solar heat flux distribution on the receiver tube has continues changes with respect to time and deformation is basically transient. Due the low speed of sun during a day and for specific time intervals, the average solar radiation could be considered constant for thermal stress and deflection analysis. Hence, in this study, thermal gradients as well as thermal stresses in the absorber tube are numerically investigated in quasi steady condition. Due to the wide changes of solar radiation during a year, computations are performed for four specific days of Spring Equinox, Summer Solstice, Autumnal Equinox and Winter Solstice. To compute solar heat flux distribution, SolTrace software is used and three dimensional heat flux distribution is applied as an external boundary condition to calculate temperature distribution in the absorber tube. By using Von-Misses theory, maximum equivalent of total stress is computed. Maximum deflection is evaluated for various different inlet temperatures and hot oil mass flow rates in the common range of solar thermal power plants for atypical parabolic trough collector which is under construction in Shiraz, Iran.

Peer review by the scientific conference committee of SolarPACES 2014 under responsibility of PSE AG

Keywords: Parabolic trough collectors; receiver tube; thermal stress; bending; quasi-steady.

*Corresponding author Tel.: +98-71-3230-1672; fax: +98-71-3647-4614.
E-mail address: yaghoubi@shirazu.ac.ir

Peer review by the scientific conference committee of SolarPACES 2014 under responsibility of PSE AG
doi:10.1016/j.egypro.2015.03.002

Nomenclature

Roman Letters

b	interaction coefficient	τ	transmittance of glass tube
D	diameter (cm)	ϕ	rim angle (°)
f	focal length of parabola (m)	ψ	circumferential angle (°)
h	heat transfer coefficient (W/m².K)	ω	hour angle (°)
k	thermal conductivity (W/m.K)	Ω	zenith angle (°)
L	length of absorber tube (m)		
$\dot{m}$	hot oil mass flow rate (kg/s)	**Subscripts**	
P	annulus gas pressure (mmHg)	a	surrounding air
q	heat flux (W/m^2)	cir	circumference
T	temperature (°C)	f	fluid
V	velocity (m/s)	g	glass tube
W	aperture width of parabolic trough (m)	gi	inner surface of glass tube
x,y,z	Cartesian coordinates	go	outer surface of glass tube
		in	inlet
Greek Letters		p	absorber tube
α	absorptance	pi	inner surface of absorber tube
γ	ratio of specific heats for the annulus gas	po	outer surface of absorber tube
δ	molecular diameter of annulus gas (cm)	solAbs	solar heat flux absorption
Δ	declination angle (°)		
ε	emittance	**Constants**	
θ	solar incidence angle (°)	K_b	Boltzmann constant (1.381×10^{-23} J/K)
Λ	accommodation coefficient	σ	Stefan-Boltzmann constant (5.67×10^{-8} W/m^2.K^4)
λ	mean-free-path between molecules (cm)	π	3.141593
ρ	reflectance of reflector		

1. Introduction

Parabolic trough collector (PTC) is one of the mature solar technologies for electricity production in thermal power plants. In a parabolic trough collector, the mirrors concentrate the sun rays on the receiver tube and the working fluid, flowing inside the absorber tube receives solar energy by convection heat transfer. Usually the absorber tube is enclosed by a glass tube to reduce the heat losses to surroundings [1]. As the PTCs are designed to operate under extremely non-uniform heat flux and cyclic weather conditions, the absorber tube will be subjected to high temperature gradients and large deflections. In some cases high temperature gradients will generate large thermal stresses which may cause the deflection of absorber tube, and consequently the rupture of glass tube which will result in the increase of heat loss [2]. Fig.1 indicates breakage the of a glass tube due to large deflection of absorber tube.

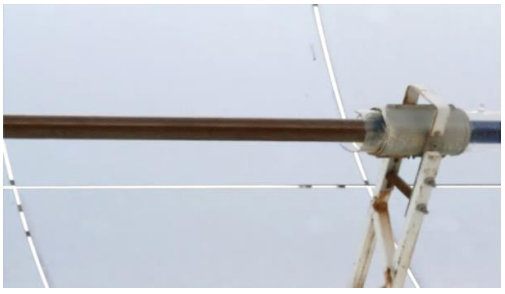

Fig.1. Typical picture of a broken glass cover due to bending of absorber tube

Temperature gradients and also stress fields in the absorber tube of parabolic trough collectors is studied recently by many researchers. Roldan et al. [3] studied numerically and experimentally the temperature distribution in the absorber tube with superheated steam as the working fluid. Lata et al. [4] tried to decrease thermal stresses and absorber tube bending by optimizing the size of the tube. Wang et al. [5] studied heat transfer in the absorber tube by inserting metal foams inside the absorber tube. They observed that by optimizing the heat transfer by use of metal foams, maximum temperature gradient on the outer surface of absorber tube is decreased by about 45% which decreases thermal stresses substantially. Regarding the fact that the performance of an absorber tube with circular cross section can be increased by increasing internal heat transfer area; Reddy et al. [2] used fins inside the absorber tube to create a porous media. They observed that by selecting the best fin diameter, heat transfer rate and pressure loss can be optimized. Wang et al. [6] proposed an eccentric tube receiver on the basis of concentric tube receivers. This tube is made by placing a tube eccentric to the absorber tube. Results showed that the use of eccentric absorber tubes decreases Von-Misses stresses about 41.1%. They also studied the effects of eccentricity and oriented angle variation on the thermal stresses of the absorber tube and found that thermal stresses reduced only when the oriented angle is between 0-90 degrees, and this decrement reaches its maximum at 90 degrees. The review on the studies conducted on thermal gradient and thermal stresses shows that researchers have studied the steady state concentrated heat flux on the absorber tube with variable circumferential distribution. But the concentrated heat flux on the absorber tube is variable over the day span which makes the problem unsteady. However the rate of these changes is not very large; hence in this study the stress field induced by variable concentrated heat flux on the absorber tube is modeled in a quasi-steady condition.

2. System description

For quasi-steady state analysis of an absorber tube, a parabolic trough collector with the specification in Table 1 is modelled. The absorber tube of this collector is made of AISI 316L steel with the specification mentioned in Akbarimoosavi et al. [7]. It should be noted that in this study Behran thermal oil [8] is selected as working fluid.

Table 1. Geometrical and optical properties of the modeled collector.

Parameter	value	Parameter	value	Parameter	value
Parabolic Mirror		**Receiver Tube**			
L×W	12.18 × 5.8	D_{po}	7	τ	0.96
f	1.67	D_{pi}	6.56	α_{po}	0.94
ρ	0.873	D_{go}	12.5	ε_g	0.15
ϕ	82	D_{gi}	11	ε_{po}	0.076

3. Methodology

The methodology of this study contains three steps. At the first step the solar heat flux distribution on the absorber tube is calculated. At the second step using results of previous step as a boundary condition, temperature distribution in the absorber tube is calculated, and at the last step temperature distribution in the absorber tube is used to calculate thermal stresses and deflection of absorber tube.

3.1. Calculation of solar heat flux on the absorber tube

The SolTrace software is utilized in order to calculate solar heat flux distribution on the absorber tube. In this application two objects should be clarified. How to divide the calculation time into smaller intervals in which the variation of direct normal irradiance (DNI) can be neglected? And what is the value of DNI for each time intervals? To answer these two questions, Daneshyar [9] solar radiation model is utilized. Daneshyar model is able to calculate the time variation of DNI in each day. Fig. 2a indicates the results of Daneshyar model at the two equinoxes and also at the two solstices for the city of Shiraz (Latitude: 29.6° N, Longitude: 52.53° E), Iran. It should be mentioned that for these four days the cloud factor in Daneshyar model is considered to be zero and consequently with this assumption, from view of solar radiation the upper limit is considered.

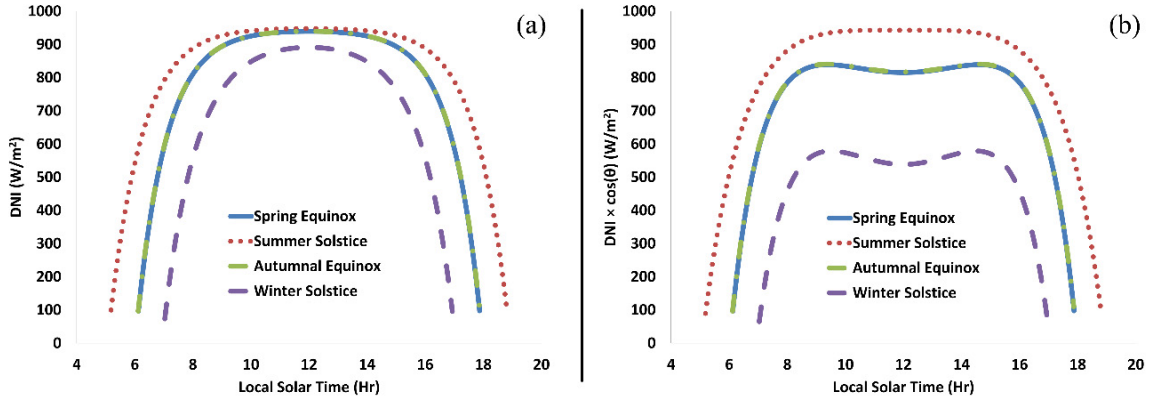

Fig. 2. (a) Hourly variation of solar radiation for Shiraz; (b) Hourly variation of solar radiation normal to aperture of an east to west tracking PTC located in Shiraz, Iran.

For a parabolic trough collector, tracking sun from east to west the incident angle is [10]:

$$\cos\theta = (\cos^2\Omega + \cos^2\Delta \sin^2\omega)^{1/2} \quad (1)$$

Using Eq. (1) and Fig. 2a, the variation of solar radiation normal to the aperture plane of a parabolic trough collector is presented in Fig. 2b. Using Fig. 2b the calculation period can be divided into smaller time steps in a way that in each sub step the variation of direct normal irradiance can be neglected which answers the first question. Also the values of DNI in each sub step can be calculated using Fig. 2a which answers the second remark. It should be mentioned that SolTrace software uses direct normal irradiance as an input to calculate the distribution of solar heat flux on the absorber tube. Based on the above statements, Table 2 indicates, the number of time steps and related values of direct normal irradiance considered for each of the four above mentioned days. Note that irradiance is symmetrical with respect to noon hour.

Table2: Steps and corresponding values of DNI (W/m^2) chosen for quasi-steady analysis, Shiraz, Iran.

Local Solar Time	Spring Equinox	Summer Solstice	Autumnal Equinox	Winter Solstice
12:00-13:30	936	942	936	883
13:30-14:00				858
14:00-14:30	916		916	831
14:30-15:00				790
15:00-15:15	888	912	888	745
15:15-15:30				705
15:30-15:45	853		853	655
15:45-16:00				592
16:00-16:15	814	874	814	512
16:15-16:30	778		778	415

Based on the measurements of Shiraz solar power plant [8], the steady state condition for inlet temperature of hot oil is achieved around solar noon. Hence with the aim of comparing the future measurements, the start point of analysis is taken to be noon hour. Also due to rapid reduction of DNI in the Shiraz solar thermal power plant around 16:30 solar time, this time is taken as the end point of computations.

3.2. Calculation of temperature distribution in the absorber tube

In order to reduce the computational costs, concept of thermal resistance [11] is used to calculate thermal losses from the surface of the absorber tube. Fig. 3 schematically shows the thermal resistance model from the surface of the absorber tube to the surrounding.

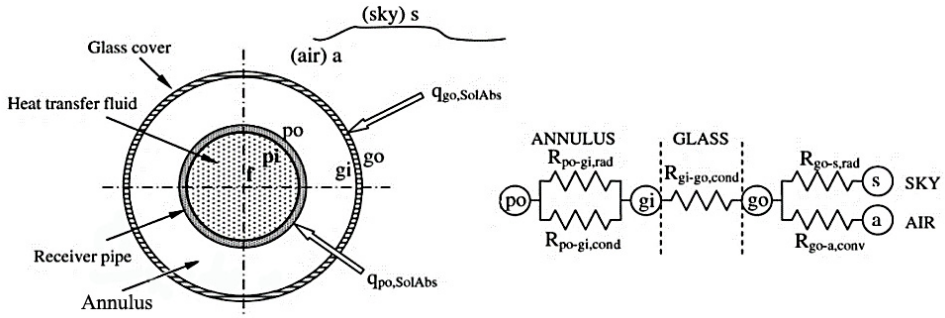

Fig. 3. Thermal resistance network for the cross-section of a receive tube.

According to Fig. 3, heat transfer in the annulus space occurs in the form of radiation and molecular conduction as indicated in Eq. (2). Heat loss passes through the glass thickness by Eq. (3) and by radiation to the sky and convection to the ambient air from the outer surface of the glass tube as presented by Eq. (4). Hence for a collector of length L, heat loss is as follows:

$$Q_{loss} = \pi D_{po} L h_f \left(T_{po} - T_{gi}\right) + \frac{\pi D_{po} L \sigma \left(T_{po}^4 - T_{gi}^4\right)}{\frac{1}{\varepsilon_{po}} + \frac{1-\varepsilon_g}{\varepsilon_g}\left(\frac{D_{po}}{D_{gi}}\right)} \tag{2}$$

$$Q_{loss} = \frac{2\pi k_g \left(T_{gi} - T_{go}\right)}{\ln\left(\frac{D_{go}}{D_{gi}}\right)} \tag{3}$$

$$Q_{loss} = \pi D_{po} L h_a \left(T_{go} - T_a\right) + \varepsilon_g \pi D_{go} L \sigma \left(T_{go}^4 - T_{sky}^4\right) - q_{go-SolAbs} \tag{4}$$

Equations (2-4) can be solved by starting with an estimate for T_{go} (which will be closer to T_a than T_{po}) and calculating the heat loss from, Eq. (4). By substituting this loss into, Eq. (3), T_{gi} can be obtained. At this step the heat loss is updated from Eq. (2) and compared with the one calculated before from Eq. (4) to check the validity of the initial guess. This procedure is repeated until the two heat losses become nearly equal. In Eq.(2), h_f presents the molecular conduction heat transfer coefficient and is calculated using the following relations [12]:

$$h_f = \frac{k_g}{\frac{D_{po}}{2}\ln\left(\frac{D_{gi}}{D_{po}}\right) + \lambda b \left(\frac{D_{gi}}{D_{po}} + 1\right)} \tag{5}$$

$$b = \frac{2-\Lambda}{\Lambda}\left[\frac{9\gamma - 5}{2\left(\gamma + 1\right)}\right] \tag{6}$$

$$\lambda = \frac{K_B\left(\overline{T}_{po-gi}\right)}{\sqrt{2}\pi P \delta^2} \tag{7}$$

In Eq. (4) h_a indicates the convection heat transfer coefficient. This coefficient depends on natural or forced convection around the glass tube and it is calculated from correlations which proposed by [13, 14] respectively. In Eq. (4), T_{sky} is approximated as T_a-8°C and ambient temperature (T_a) and wind speed (V) are required to calculate h_a. The averaged values of these two parameters are taken from the time intervals under study. By calculating heat losses from the surface of the absorber tube, there is no need to model the glass tube and annulus space in numerical analysis. Hence the computational domain involves only the absorber tube and the fluid flowing inside it and the heat losses can be used as a boundary condition on the outer surface of the absorber tube. Fig. 4 shows the

computational domain and the grid used to solve the governing equations. After performing a grid independent study based on the variation of heat transfer coefficient on the inner surface of the absorber tube, a grid of 2,500,000 cells is chosen for calculation domain. In order to investigate the temperature gradient in the absorber tube, with the assumption of three dimensional, incompressible, steady state and turbulent flow, a finite volume code is utilized to solve mass, momentum and energy equation [15]. Also in order to estimate Reynolds stresses, the k-ε model [16] is utilized.

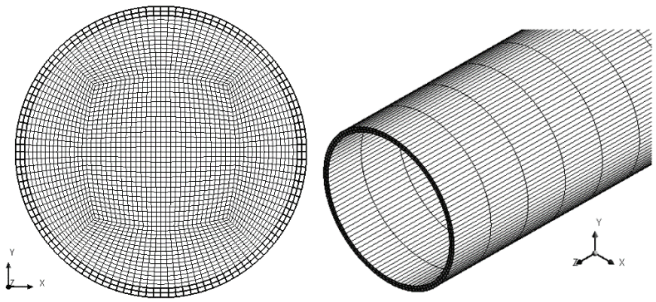

Fig. 4. A view of grid used to solve governing equations using finite-volume method.

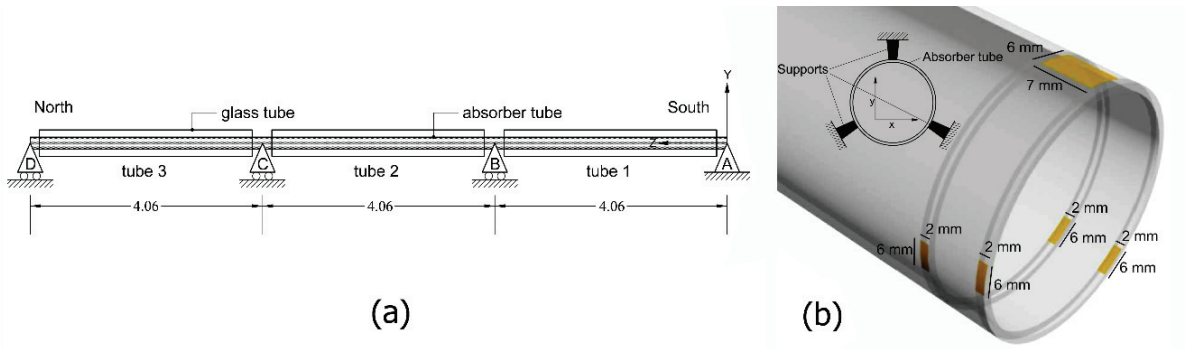

Fig. 5. (a) Schematic of supports used to hold the absorber tube in focal line of parabola; (b) Schematic of actual contact area between absorber tube and supports

3.3. Calculation of thermal stresses in the absorber tube

Fig. 5a schematically shows the four supports used to hold the absorber tube in the focal line of the parabola. As it is presented in Fig. 5a, displacement of support A is fixed in all directions however the other supports are allowed to move along the Z axis freely. Also all the supports are allowed to rotate around the X axis freely. Fig. 5b also schematically shows the actual contact area between absorber tube and supports. After calculation of temperature distribution in the absorber tube in each sub step, the temperature distribution is imported into a finite-element code as a thermal load in order to calculate the thermal stress and deflection of absorber tube. In this study thermo elastic equations [17] are solved with the aim of calculating thermal stress fields and deflections for the absorber tube. It should be mentioned that steady state situation is considered in each sub step, hence the energy and the stress-strain equations become decoupled [17].

4. Results and discussion

In this study each day period is divided into proper time steps as shown in Table 2 and the distribution of solar heat flux on the absorber tube is calculated for each of these time steps. Solving the governing equations, temperature distribution in absorber tube is calculated and using temperature distribution and solving the thermo elastic equations, thermal stress and deflection of absorber tube is calculated for each day.

4.1. Solar heat flux on the absorber tube

Figs. 6 show the solar heat flux on the absorber tube at first interval corresponding to each day. As the location of sun at the spring and the autumnal Equinox is equal [10] and also by assuming zero cloud factor in the Daneshyar model [9], the solar heat flux at the spring Equinox is equal to the autumnal Equinox. Based on Fig. 6, at winter Solstice, a considerable length of absorber tube doesn't receive the concentrated solar heat flux. This length reaches to approximately 2 meters. This length for summer Solstice is minimum and approximately 20 centimeters. This fact could be explained by the height of sun at different seasons.

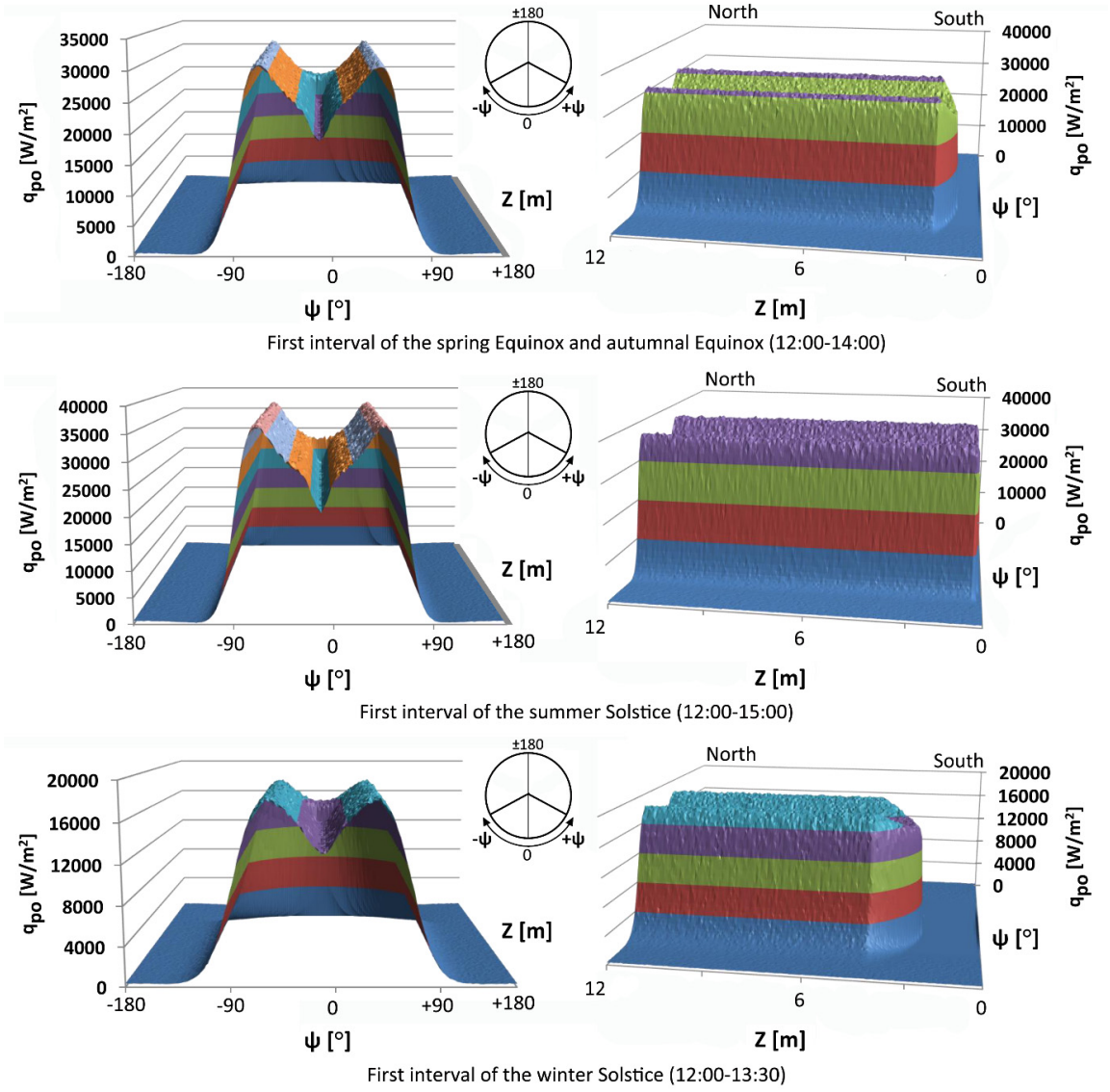

Fig. 6. Three dimensional solar heat flux distribution on the absorber for different considered days

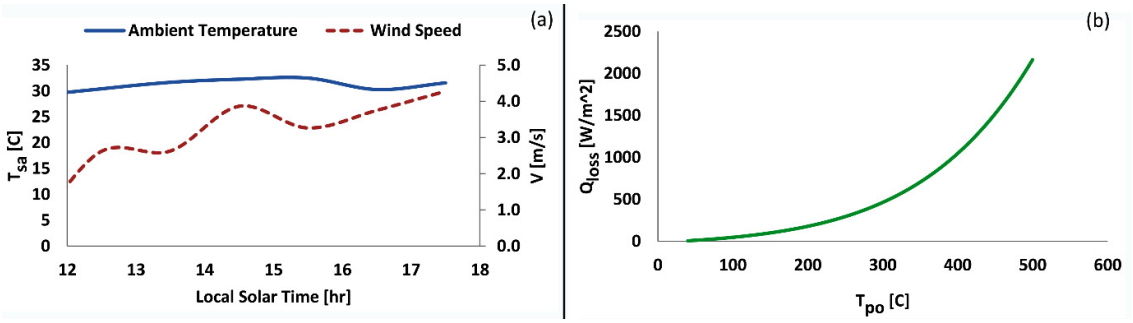

Fig. 7. (a) Variation of average ambient temperature and wind speed at autumnal Equinox [18]; (b) Heat losses from the surface of the absorber tube at first interval of autumnal Equinox (12:00-14:00)

4.2. Temperature distribution in the absorber tube

In order to calculate heat losses from the outer surface of the absorber tube, the climate data taken from [18] is utilized. Fig. 7a indicates the ambient temperature and wind speed for autumnal Equinox and Fig. 7b shows the corresponding heat loss at first interval of autumnal Equinox. For the specified collector, mass flow rate and inlet temperature may have different values. For a condition near to the design specification, these two parameters are considered to be 1.5 kg/s and 250℃ respectively. Fig. 8 presents temperature distribution at different sections of the absorber tube along the length of the absorber) at the first interval of autumnal Equinox (12:00-14:00) for the specified oil mass flow rate and inlet temperature. Fig. 8 indicates that, the circumferential temperature gradients enlarge as the hot oil passes through the first section of the absorber tube. It should be noted that in Fig. 8, $\Delta T_{p,\,cir}$ is defined as the maximum absorber tube circumferential temperature difference.

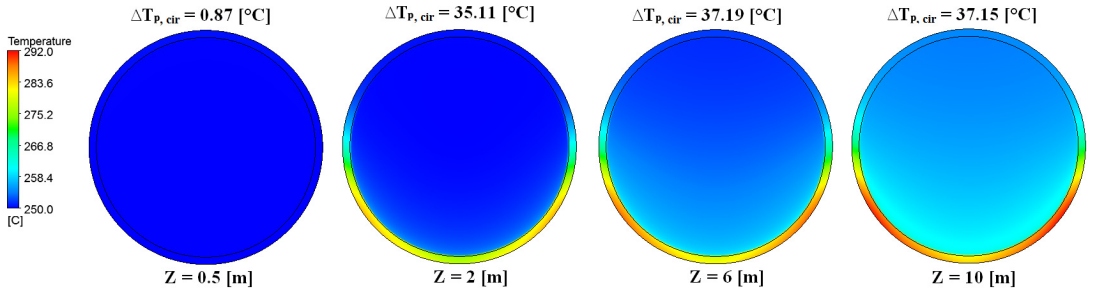

Fig. 8. Temperature distribution at cross section of the absorber tube at first interval of autumnal Equinox (12:00-14:00) $\dot{m}$ =1.5 kg/s and T_{in}= 250 °C

4.3. Analysis of deflection of the absorber tube

Fig. 9shows daily variation of maximum deflection of the absorber tube for different inlet temperature and mass flow rates at the four mentioned days. Comparing graphs of Fig. 9indicates that for a constant mass flow rate, increasing inlet temperature caused reduction of maximum deflection of the absorber tube. For instance at Fig. 9c, for $\dot{m}$=1.5 kg/s, by increasing inlet temperature from 200℃ to 300℃, the maximum deflection of absorber is reduced about 41 percent. Comparing graphs of Fig. 9also indicates that for a constant inlet temperature, increasing mass flow rate reduces maximum deflection of tube. For instance at Fig. 9c, for T_{in}=200℃, increasing mass flow rate from 1 kg/s to 1.5 kg/s causes the reduction of about 24 percent in the absorber tube maximum deflection. Increase of convection heat transfer coefficient and consequently improvement of heat transfer between tube and hot oil is the main reason of this reduction. Using Newtonian law of cooling the values of convection coefficient as indicated in Fig. 9 are calculated incorporating the weighted average of heat flux and absorber's inner surface temperature and using average of the oil inlet and outlet temperature as the reference temperature.

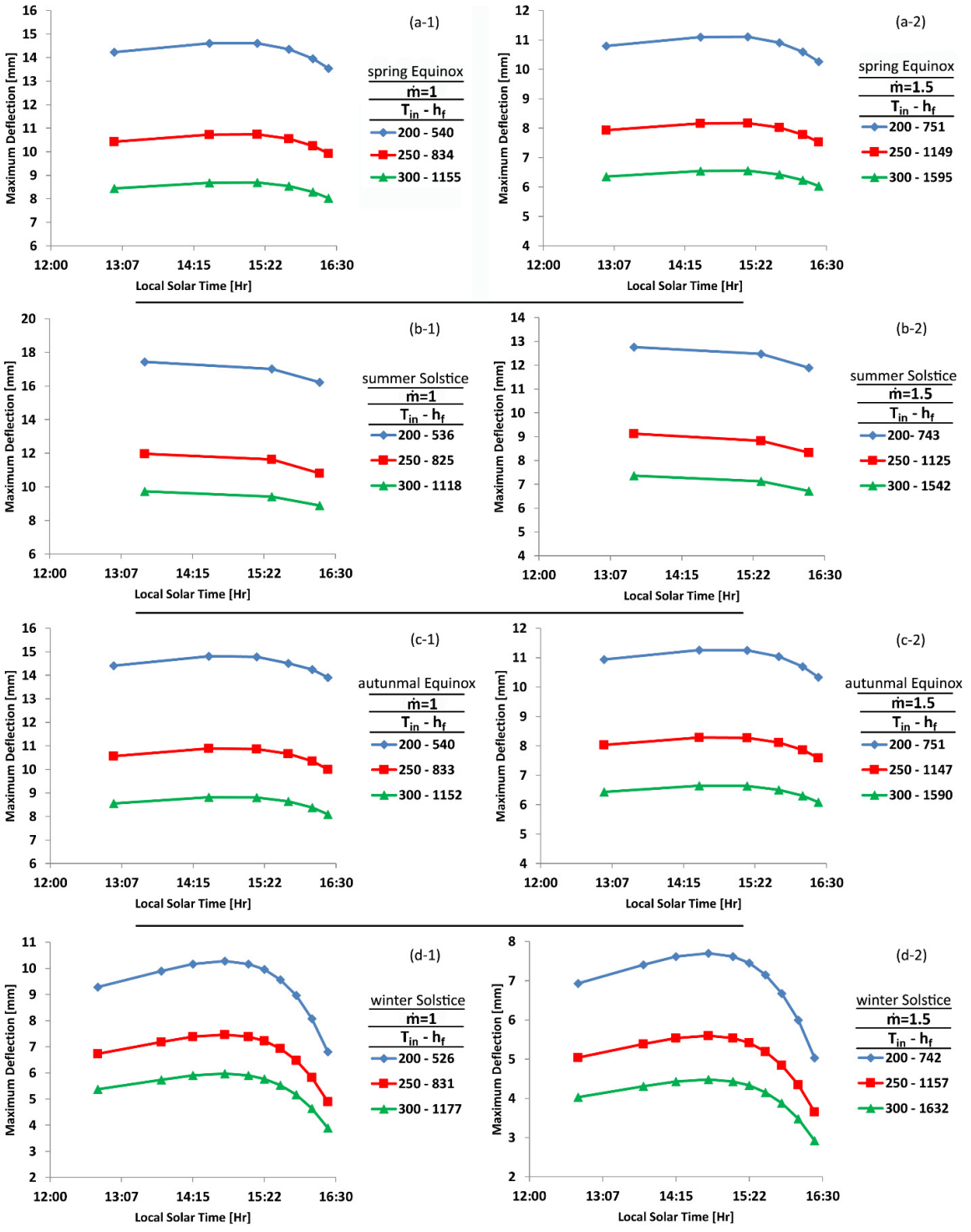

Fig. 9. Maximum deflection of the absorber tube for different hot oil flow rates

Interesting results are the form of tube deflection and the location of maximum deflection of absorber tube. Fig. 10 indicates typical deformation of absorber tube for T_{in}=250°C and ṁ=1.5 kg/s at autumnal Equinox. Based on Fig. 10, the maximum deflection of absorber occurs at a location between support C and D of Fig. 5a. Also the tube at the fixed end has higher variation of deflection with respect to time.

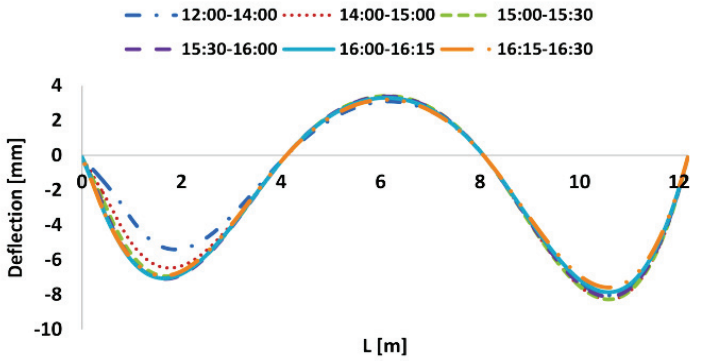

Fig. 10. Deflection of the absorber tube at various intervals, for autumnal Equinox

5. Conclusion

The quasi-steady analysis of deflection of absorber tube of a parabolic trough collector shows that:

1- Solar heat flux along the absorber tube changes considerably at winter Solstice, while its distribution is almost uniform for the other seasons.
2- Absorber tube circumferential temperature variation is a function of tube axis position. It is low at entrance, while it reaches to ΔT_{max}=37.19°C for typical condition of ṁ=1.5 kg/s and T_{in}=250°C, during the autumnal Equinox.
3- Circumferential temperature difference reduces by increasing hot oil temperature considerably.
4- Tube deflection varies along the tube length. It is maximum between tube supports. The free end section has the largest deflection.
5- Deflection has slight variation with respect to time, mostly for the fixed end tube.
6- Deflection of tube for summer Solstice is higher than other specified days.

Acknowledgements

This study is supported by Iran's National Elites Foundation.

References

[1] Almanza R, Lentz A, Jimenez G. Receiver behavior in direct steam generation with parabolic troughs. Solar Energy 1998;61:4-275-8.
[2] Reddy K S, Kumar K R, Satyanarayana G V. Numerical investigation of energy-efficient receiver for solar parabolic trough concentrator. Heat Transfer Engineering 2008;29:11-961-72.
[3] Roldán M I, Valenzuela L, Zarza E. Thermal analysis of solar receiver pipes with superheated steam. Applied Energy 2013;103-73-84.
[4] Lata J M, Rodríguez M, de Lara M Á. High flux central receivers of molten salts for the new generation of commercial stand-alone solar power plants. Solar Energy Egineering 2008;130:2-021002.
[5] Wang P, Liu D Y, Xu C. Numerical study of heat transfer enhancement in the receiver tube of direct steam generation with parabolic trough by inserting metal foams. Applied Energy 2013;102-449-60.
[6] Wang F, Shuai Y, Yuan Y, Yang G, Tan H. Thermal stress analysis of eccentric tube receiver using concentrated solar radiation. Solar Energy 2010;84:10-1809-15.
[7] Akbarimoosavi S M, Yaghoubi M. 3d thermal-structural analysis of an absorber tube of a parabolic trough collector and the effect of tube

deflection on optical efficiency. Energy Procedia 2014;49-2433-43.
[8] Rahmatmand A, Yaghoubi M, Raesi M, Niknia I, Kanan P. Experimental analysis of shiraz solar thermal power plant performance during 2009-2011. Optoelectronics and Advanced Materials 2013;15:5-571 - 7.
[9] Daneshyar M. Solar radiation statistics for iran. Solar Energy 1978;21:4-345-9.
[10] Duffie J A, Beckman W A. Solar engineering of thermal processes: John Wiley & Sons; 2013.
[11] Incropera F P. Fundamentals of heat and mass transfer: John Wiley & Sons; 2011.
[12] Dushman S. Scientific foundations of vacuum technique. 2 ed. Lafferty J M, editor. New York: J. Wiley and Sons; 1962.
[13] Churchill S W, Chu H H. Correlating equations for laminar and turbulent free convection from a horizontal cylinder. International Journal of Heat and Mass Transfer 1975;18:9-1049-53.
[14] Zukausras A. Heat transfer from tubes in crossfiow. Advances in Heat Transfer 1973;8-93.
[15] Bejan A. Convection heat transfer. Hoboken (N. J.): J. Wiley & Sons; 2013.
[16] Wilcox D C. Turbulence modeling for cfd: DCW industries La Canada, CA; 1998.
[17] Nye J F. Physical properties of crystals: Clarendon Press; 1985.
[18] Weather history for shiraz, iran | weather underground [cited 2014]. Available from: http://www.wunderground.com/history/airport/OISS.